An elastic-spring-substrated nanogenerator as an active sensor for self-powered balance†

Long Lin,[a] Qingshen Jing,[ac] Yan Zhang,[a] Youfan Hu,[a] Sihong Wang,[a] Yoshio Bando,[b] Ray P. S. Han[c] and Zhong Lin Wang*[ab]

We report on a novel design of a piezoelectric nanogenerator that is monolithically integrated onto an elastic spring by growing ZnO nanowire arrays on the surface of the spring. Under a cyclic compressive force applied to the spring, the nanogenerator produced a stable AC output voltage and current, which are linearly responding to the applied weight on the spring. By conjunction of the experimental data with finite element simulation, we show that the output open-circuit voltage of the nanogenerator can serve as an active sensor for a self-powered weight measurement system. By active sensor we mean that the sensor automatically gives an electric output signal without applying an external power source, which can be used to directly quantify the mechanical triggering applied onto the nanogenerator.

Introduction

Wireless sensor networks play a key role in various fields, including health/environment monitoring, defense technology, and artificial skins.[1–4] Traditional wireless sensors require a battery as a power source, and the battery might lead to problems such as adding weight to the whole system, limited life time, high cost of replacement, or potential hazard to the environment. To solve these problems, battery-free self-powered sensors, which could scavenge energy from the environment as the power source, are highly desirable. In this regard, the piezoelectric nanogenerator (NG) based on semiconductor nanostructures has been developed since 2006,[5] which can convert mechanical vibration into electricity *via* the piezoelectric effect of one dimensional nanostructures, like ZnO,[6–8] GaN,[9] polyvinylidene fluoride (PVDF),[10] and lead zirconate titanate (PZT).[11] More recently, NGs were used as self-powered pressure/strain sensors to actively detect the mechanical vibrations

Broader context

Wireless sensor networks play a key role in various fields, including health/environment monitoring, defense technology, and artificial skins. In this regard, the recently developed active sensor can be used to directly quantify the mechanical triggering applied onto a piezoelectric nanogenerator without applying an external power source. Many applications have been demonstrated in this field including heart-beating pulse diagnosis, tyre pressure/speed measurement, wind speed detection, and transportation control system. The research presented in this paper introduces the fabrication and characterization of a spring-substrated nanogenerator based on the hydrothermal growth of a ZnO nanowire film on a spring. The nanogenerator shows a stable output and both the output voltage and current display a linear relationship with the weight loaded on the spring. Thus, the nanogenerator can be utilized as an active mechanical sensor for measuring the weight applied onto the spring. This work is a new step towards practical applications of nanogenerators as self-powered sensors.

without using a battery.[12] Applications of the NG-based active sensors have been demonstrated in various fields, such as heart-beating pulse diagnosis,[13] tyre pressure/speed measurement,[14] wind speed detection,[15,16] and transportation control system.[17]

An elastic spring is a commonly employed mechanical accessory in lots of equipment and automobiles, and it is one of the most traditional balances used for measuring weight in reference to the extended length of the spring. In this work, a spring-substrated nanogenerator (SNG) was fabricated to accomplish the monolithic integration of an active sensor device onto a mechanical component. The ZnO nanowires (NWs) were densely grown on the surface of the spring by the wet chemical approach. The SNG was fabricated by applying polymer passivation onto the textured ZnO NW film and silver electrode on the composite structure. The SNG showed a stable output open-circuit voltage and short-circuit current under a cyclic compressive force. Both the output voltage and current had a linear relationship with the weight loaded onto the spring, thus, the NG was utilized as an active mechanical sensor for measuring the weight applied onto the spring. The applicability of the active

[a]*School of Material Science and Engineering, Georgia Institute of Technology, Atlanta, Georgia, 30332-0245, USA. E-mail: zlwang@gatech.edu*

[b]*International Center for Materials Nanoarchitectonics, National Institute for Materials Science, 1-1 Namiki, Tsukuba, 305-0044, Japan*

[c]*College of Engineering, Peking University, Beijing, 100871, China*

† Electronic supplementary information available. See DOI: 10.1039/c3ee00107e

1164 | *Energy Environ. Sci.*, 2013, **6**, 1164–1169

This journal is © The Royal Society of Chemistry 2013

sensor was systematically analyzed for different parameters. This work is a new step towards practical applications of nano-generators as self-powered sensors.

Results and discussions

The structure and general working principle of the SNG are schematically shown in Fig. 1a–c. Compressive springs with variable sizes were selected as the skeletons of the SNG devices. The helix-shaped spring surface was composed of high carbon steel, which was taken as the substrate for the growth of ZnO NWs and was also employed as the inner electrode due to the conductive nature of the steel. The ZnO NWs were grown by the wet chemical approach[18,19] on the treated spring surface (see the Experimental section for details). The surface morphology of the ZnO NWs is presented by the scanning electron microscopy (SEM) images in Fig. 1d and e. The NWs were uniformly grown on the spring (Fig. S1†) and densely packed as a textured film with the *c*-axes of the NWs pointing outward.[18] The as-synthesized NW film was coated with polymethyl methacrylate (PMMA) as a buffer layer[8] and deposited with silver as the outer electrode. Both the inner and outer electrodes were connected to the external

measurement circuit by copper electric leads, and the whole device was encapsulated with polydimethylsiloxane (PDMS) to protect the electrode.

In the measurement for the output performance of the SNG, one end of the spring was fixed onto a three-dimensional stage; meanwhile a mechanical linear motor was employed to apply a periodic longitudinal compressive force to the SNG. As the compressive force is applied onto the spring, the strain-induced piezoelectric potential (piezopotential) in ZnO will be created and drive the electrons flowing in the external load until the accumulated electrons reach equilibrium with the piezopotential; once the applied force is released, the piezopotential diminishes and the accumulated electrons will flow back in the opposite direction, which leads to an AC current. With an applied compressive force of 15.2 N (the corresponding displacement of the spring is 10 mm), for a spring with spring constant of 1.52 N mm^{-1}, the output open-circuit voltage and short-circuit current of the SNG was ~0.23 V and 5 nA, respectively, as displayed in Fig. 2a and b. The stability of its output performance was also tested through continuously loading and unloading the periodic force for three days at a frequency of 0.32 Hz. From Fig. 2c and d, it can be found that the output of the SNG only showed a decay of 3–4% after three days of continuous working (corresponding to ~80 000 cycles), owing to the high flexibility of the ZnO NWs and thus the high robustness of the SNG device. The stability of the SNG's output ensures its application as an active mechanical sensor, which will be discussed later.
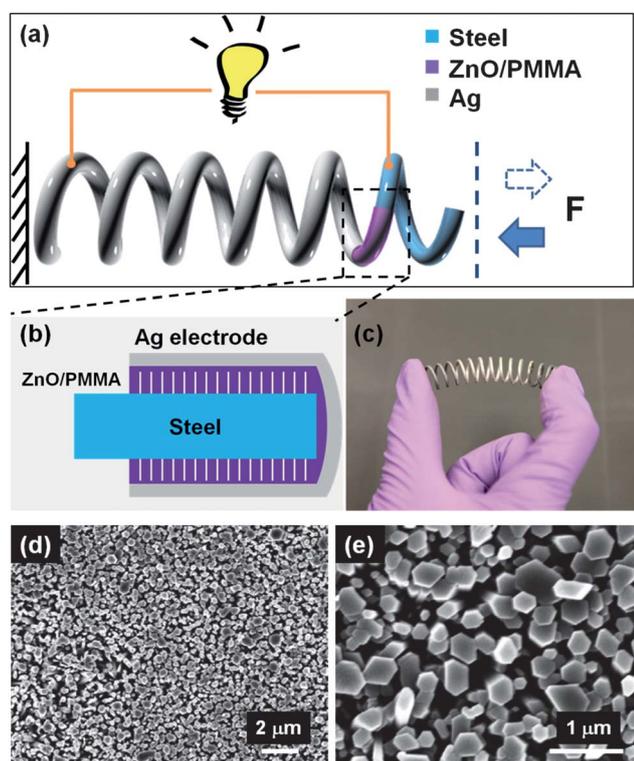
Fig. 1 (a) Schematic structure of the spring-substrated nanogenerator, in which a textured piezoelectric ZnO nanowire film is grown on the surface of the elastic wire. (b) A cross-sectional schematic illustration of the nanogenerator showing its detailed structure, which is composed of a steel spring (substrate and inner electrode), ZnO nanowire film, PMMA insulating layer, as well as the outer Ag electrode. (c) A photograph of the spring-substrated nanogenerator. (d) Low magnification SEM image of the ZnO nanowire film indicating the uniformity of the NW film. (e) High magnification SEM image of the ZnO NW film showing the hexagonal structure of the ZnO nanowires.
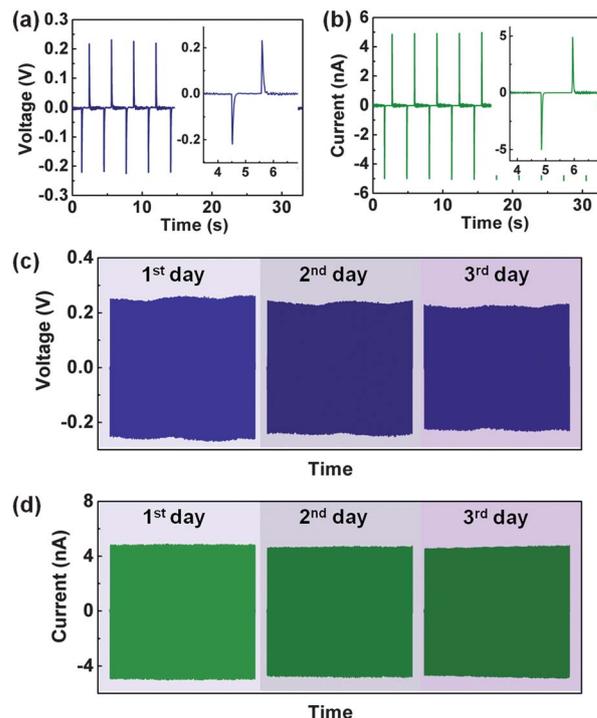
Fig. 2 Electrical output performance of the SNG. (a) Open-circuit voltage and (b) short-circuit current of the SNG. The insets are the enlarged views of the open-circuit voltage and short-circuit current. (c and d) Stability tests of the (c) output voltage and (d) current of the SNG with continuous working for three days at a frequency of 0.32 Hz. The data presented contain 200 cycles of the output voltage/current for each day.

To achieve a fundamental understanding and offer guidance for the practical design of the SNG, its working mechanism was analyzed using a finite element calculation. Due to the relative complexity of the stress distribution on the surface of the spring when loaded with a longitudinal force, only the tangent force term was considered as a contribution to the piezopotential across the ZnO NW film. In the numerical calculation, a segment of the spring as well as the corresponding ZnO NW film was selected for the calculation. At a displacement of 10 mm for the spring deformation, the tangent force applied to the selected segment of the spring/ZnO NW composite was calculated based on the following relationships:

$$F_0 = kx \qquad (1)$$

$$F = F_0 \cdot \sin \alpha \qquad (2)$$

here, F_0 is the total longitudinal force, which is proportional to the displacement of the spring (x), F is the tangent force that will act parallel to the ZnO film, and α is the declination angle of the spring, and their relationship is schematically illustrated in Fig. S2.† With a spring constant of $k = 1.52$ N mm^{-1}, and the declination angle of $\alpha = 0.22$ radian, it could be calculated that the applied tangent force is $F = 3.3$ N. Under this applied force, the potential distribution across the thickness direction of the ZnO NW film was calculated from finite element analysis, as given in Fig. 3a. The calculated potential difference between the top electrode and the bottom spring electrode is 0.27 V, which is consistent with the measured open-circuit voltage under the same condition. Moreover, the relationship between the strain-induced piezoelectric potential and the displacement of the spring was also calculated in the same way and is displayed in Fig. 3b. The piezoelectric potential shows a linear relationship with the displacement of the spring, which is equivalent to the applied strain or force on the ZnO NW film. Based on this result, the SNG could be employed to serve as an active mechanical sensor, by which the information of the applied force could be derived from the measured output open-circuit voltage and/or short-circuit current of the SNG without applying an external power source. The expected sensitivity was 27 mV mm^{-1} from the result of Fig. 3b. A more detailed analysis of the periodical current flow behavior of the SNG under a cyclic compressive force is illustrated in Fig. 3c and d. As observed from the enlarged diagram showing a full cycle of the output current of the SNG (Fig. 3c), it can be divided into four stages corresponding to the different applied force conditions: (I) the spring was fixed at one end, and its free end was applied with a compressive force by a linear motor from its original position. The strain-induced piezopotential will drive the electrons flowing in the external circuit, until the accumulated electrons reach equilibrium with the piezopotential. Thus, a current peak was measured. (II) The compressive force reached its maximum value and kept constant, and there was no current flowing in the external circuit, which was reflected by the inset of Fig. 3c (top left). (III) As the compressive force was released, the piezopotential vanished and the accumulated electrons would flow back through the external circuit to the original electrode, and a
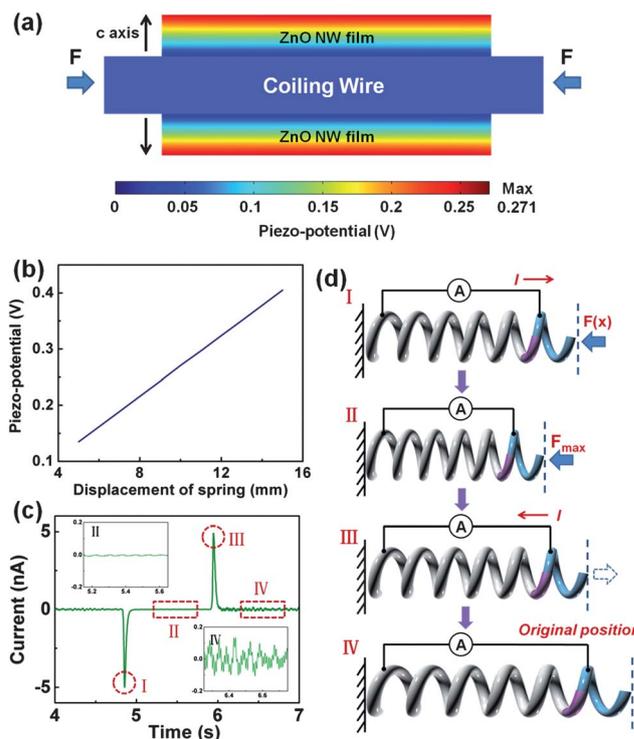
Fig. 3 (a) The calculated piezopotential distribution in the ZnO nanowire film with an applied compressive force. Since the size of the spring is a lot larger than the size of the nanowire and the ZnO film thickness, the calculation was done for a simplified case that the 3D shape of the spring was not considered. This result only gives the potential distribution in a segment of the spring-substrated nanogenerator. (b) The calculated piezopotential across the ZnO nanowire film as a function of the displacement of the spring. (c) The detailed analysis of the output current of a SNG, which consists of four steps. (d) The schematic diagrams displaying the measurement process of the spring-substrated nanogenerator and an explanation of the AC output current.

current peak with the opposite polarity was measured. (IV) At the end of the cycle, the accumulated electrons had fully flowed back, and the current flow tended to be zero. However, different from stage (II), the linear motor was fully removed from the spring in this stage, and the free vibration of the spring would induce an oscillation in the output current of the SNG, which is also shown in the inset of Fig. 3c (bottom right), indicating that the SNG functioned as a self-powered vibration sensor for monitoring buildings or bridges.[20]

Since the displacement of the spring has a direct relationship with the applied force by Hooker's Law, the output voltage and current of the SNG as a function of the displacement of the spring were measured to demonstrate the performance of the SNG as an active mechanical sensor. Fig. 4a and b show the measured magnitude of the output open-circuit voltage and short-circuit current with a series of displacements ranging from 5 mm to 15 mm. The measurement result clearly indicates that both the open-circuit voltage and short-circuit current increase with the displacement of the spring. Through statistical analysis of the measured data, it was calculated that the voltage and current sensitivity of the active sensor was 7 mV mm^{-1} and 0.44 nA mm^{-1}, respectively (Fig. S3†). Based on these results, the application of the active sensor as a self-powered
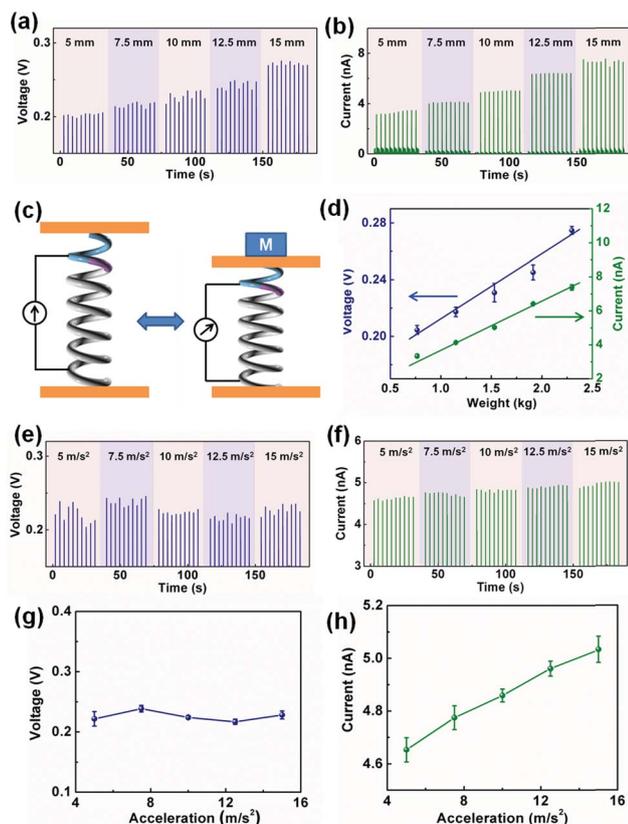
Fig. 4 Electrical measurement of the active mechanical sensor for self-powered weight measurement. (a and b) Output open-circuit voltage and short-circuit current of the active sensor as a function of the displacement of the spring. (c) Schematic illustration showing the working mode of the active mechanical sensor for self-powered weight measurement. (d) Linear relationship between the output and loaded weight on the spring-substrated nanogenerator. (e and f) The measured open-circuit voltage and short-circuit current as a function of the acceleration of the linear motor by which the external force was loaded. (g and h) The statistical relationship between the output voltage/current and the acceleration of the linear motor.

and to validate the measured working curve of the active sensor. Since loading of the applied force is a dynamic process, the loading rate dictated by the acceleration of the motor is one of the most important parameters to study. Ideally, the open-circuit voltage should merely depend on the strain-induced piezopotential and thus the magnitude of the applied force; while the short-circuit current is not only dependent on the amount of charges transferred, but also affected by the charge flow rate, which is decided by the acceleration of the loaded force. Fig. 4e and f show the measured open-circuit voltage and short-circuit current as a function of the acceleration of the linear motor (the external force was kept constant at 15.2 N), and the voltage/current-acceleration relationship was statistically analyzed and summarized, as shown in Fig. 4g and h. The results are consistent with the theoretical expectation, in which the open-circuit voltage is generally independent of the acceleration, but the short-circuit current shows a slightly increasing trend as the acceleration increases. Therefore, it clearly indicates that the open-circuit voltage is a more accurate and reliable way for the self-powered weight measurement. The short-circuit current, though changing with loading rate, could give more detailed information about the dynamic process of the applied force.

Besides, the effect of spring size was also studied by using a smaller spring as the substrate for the fabrication of SNG. The output voltage and current with variable spring displacements were measured and are shown in Fig. S5 and S6.† The output of the SNG is smaller as expected, but both the output voltage and current also have a linear relationship with the spring

balance was proposed, as illustrated in Fig. 4c. The SNG was placed vertically with a tiny plate on its top (the weight of the plate and the induced deformation of the spring were negligible compared to the heavy object for measurement), and the heavy object for measurement was then placed on top of the plate. The induced output voltage/current could be measured, from which the information of the weight of the object was derived. Fig. 4d shows the linear relationship between the output voltage/current responses and the equivalent weight calculated from the spring displacement. It could also be calculated that the voltage and current sensitivity for the weight measurement were 45 mV kg^{-1} and 2.8 nA kg^{-1}, respectively. The proposed self-powered operation of the active sensor is also schematically illustrated in Fig. S4,† with its "working mode" for signal detection and "standby mode" for energy scavenging.

The output of the SNG is mainly determined by the external force applied on the spring; however, it might also be affected by other parameters like the loading rate of the force, the spring size and the working frequency. Therefore, controlled experiments are indispensable to exclude other possible interferences

Fig. 5 The measured output voltage of a smaller SNG with variable frequencies of the loading force, but the displacement of the spring was kept at a constant.

This journal is © The Royal Society of Chemistry 2013

Energy Environ. Sci., 2013, **6**, 1164–1169 | **1167**

displacement, which means that the working principle of the SNG as an active sensor is valid regardless of the size limitation of the spring in practical applications. Being analogous to the acceleration of the linear motor, the frequency of the applied impact should have little effect on the output open-circuit voltage, while the output short-circuit current is more sensitive to the impact frequency. In this case, the frequency test of the open-circuit voltage is given in Fig. 5 and indicates that the frequency of the impact has little influence on the magnitude of the output open-circuit voltage especially in the low frequency range, which further confirms the effectiveness of using the output voltage as the signal for the active sensor.

Conclusion

In summary, by growing nanowire films of ZnO on the surfaces of the elastic wire for a spring, a spring-based nanogenerator has been demonstrated as an active sensor for measuring the weight applied onto the spring without the use of an external power source. Both the output voltage and current displayed a linear relationship with the equivalent applied weight to the spring, and the weight measurement was validated by comparison with other factors like loading rate of the force, spring size, and impact frequency. Our study shows that the output voltage of the nanogenerator could be utilized as an active sensor signal for a self-powered weight measurement system, which can be further employed in transportation monitoring.

Experimental section

Synthesis of the ZnO nanowire film

The selected spring was 2.5 inch in length and 0.048 inch in wire diameter. The ZnO nanowires were grown by the wet chemical approach on the surface of the spring. Before the growth, the spring was treated with 0.1 mol L^{-1} of hydrochloric acid (HCl, Alfa Aesar) solution for 5 min to remove the surface oxidation layer. The surface of the as-treated spring was coated with a ZnO seed layer (150 nm) by RF sputtering (PVD 75, Kurt J. Lesker). In the next step, the spring was placed in the nutrient solution consisting of zinc nitrate and hexamethylenetetramine (HMTA, Sigma Aldrich) with equal concentration (0.1 mol L^{-1}). The NW growth took place in a mechanical converter oven (Yamato DKN400, Santa Clara) at 95 °C for 5 hours. As soon as the growth was complete, the samples were rinsed in distilled water to remove the chemical residuals. The size of the smaller spring selected for the controlled experiment was 2 inch in length and 0.029 inch in diameter. The detailed information about the springs is summarized in Table S1.†

Electrical measurement of the output of the SNG

The measurement of the open-circuit voltage and short-circuit current of the SNG was carried out using an SR560 low noise voltage amplifier and SR570 low noise current amplifier (Stanford Research Systems), respectively. A mechanical linear motor (Labworks Inc., ET-132-203) was utilized to apply a cyclic compressive force onto the SNG.

Numerical calculation of the piezopotential across the ZnO nanowire film

The numerical calculation of the piezopotential was carried out using Comsol 3.5a. Since the ZnO NWs were densely grown on the substrate, we assumed that the NWs formed a textured film. According to the growth mechanism, the c-axis of the film was chosen to point toward the top electrode. The selected segment of the textured film for calculation was 20 mm in length and 2 mm in thickness. The calculated piezopotential was expressed as the rainbow color range in the diagram. The material constants used in the calculation were: anisotropic elastic constants of ZnO: $C_{11} = 207$ GPa, $C_{12} = 117.7$ GPa, $C_{13} = 106.1$ GPa, $C_{33} = 209.5$ GPa, $C_{44} = 44.8$ GPa, $C_{55} = 44.6$ GPa, piezoelectric constants $e_{15} = -0.45$ C m^{-2}, $e_{31} = -0.51$ C m^{-2} and $e_{33} = 1.22$ C m^{-2}. The ZnO relative dielectric constants were $k_{\perp} = 7.77$ and $k_{\parallel} = 8.91$.

Acknowledgements

Notes and references

1 C. Y. Chong and S. P. Kumar, *Proc. IEEE*, 2003, **91**, 1247–1256.

2 T. Someya, Y. Kato, T. Sekitani, S. Iba, Y. Noguchi, Y. Murase, H. Kawaguchi and T. Sakurai, *Proc. Natl. Acad. Sci. U. S. A.*, 2005, **102**, 12321–12325.

3 Z. Y. Fan, J. C. Ho, T. Takahashi, R. Yerushalmi, K. Takei, A. C. Ford, Y. L. Chueh and A. Javey, *Adv. Mater.*, 2009, **21**, 3730–3743.

4 D. J. Lipomi, M. Vosgueritchian, B. C. K. Tee, S. L. Hellstrom, J. A. Lee, C. H. Fox and Z. N. Bao, *Nat. Nanotechnol.*, 2011, **6**, 788–792.

5 Z. L. Wang and J. H. Song, *Science*, 2006, **312**, 242–246.

6 R. S. Yang, Y. Qin, L. M. Dai and Z. L. Wang, *Nat. Nanotechnol.*, 2009, **4**, 34–39.

7 Y. F. Hu, Y. Zhang, C. Xu, L. Lin, R. L. Snyder and Z. L. Wang, *Nano Lett.*, 2011, **11**, 2572–2577.

8 G. Zhu, A. C. Wang, Y. Liu, Y. Zhou and Z. L. Wang, *Nano Lett.*, 2012, **12**, 3086–3090.

9 L. Lin, C. H. Lai, Y. F. Hu, Y. Zhang, X. Wang, C. Xu, R. L. Snyder, L. J. Chen and Z. L. Wang, *Nanotechnology*, 2011, **22**, 475401.

10 C. E. Chang, V. H. Tran, J. B. Wang, Y. K. Fuh and L. W. Lin, *Nano Lett.*, 2010, **10**, 726–731.

11 X. Chen, S. Y. Xu, N. Yao and Y. Shi, *Nano Lett.*, 2010, **10**, 2133–2137.

12 Z. L. Wang, *Nano Today*, 2010, **5**, 512–514.

13 Z. T. Li and Z. L. Wang, *Adv. Mater.*, 2011, **23**, 84–89.

14 Y. F. Hu, C. Xu, Y. Zhang, L. Lin, R. L. Snyder and Z. L. Wang, *Adv. Mater.*, 2011, **23**, 4068–4071.

15 R. Zhang, L. Lin, Q. S. Jing, W. Z. Wu, Y. Zhang, Z. X. Jiao, L. Yan, R. P. S. Han and Z. L. Wang, *Energy Environ. Sci.*, 2012, **5**, 8528–8533.

16 C. L. Sun, J. Shi, D. J. Bayerl and X. D. Wang, *Energy Environ. Sci.*, 2011, **4**, 4508–4512.

17 L. Lin, Y. F. Hu, C. Xu, Y. Zhang, R. Zhang, X. N. Wen and Z. L. Wang, *Nano Energy*, 2012, **2**, 75–81.

18 L. Vayssieres, *Adv. Mater.*, 2003, **15**, 464–466.

19 L. E. Greene, M. Law, J. Goldberger, F. Kim, J. C. Johnson, Y. F. Zhang, R. J. Saykally and P. D. Yang, *Angew. Chem., Int. Ed.*, 2003, **42**, 3031–3034.

20 A. F. Yu, P. Jiang and Z. L. Wang, *Nano Energy*, 2012, **1**, 6.

This journal is © The Royal Society of Chemistry 2013

Energy Environ. Sci., 2013, **6**, 1164–1169 | **1169**